

# Two conserved modules of *Schizosaccharomyces pombe* Mediator regulate distinct cellular pathways

Tomas Linder<sup>1</sup>, Nina N. Rasmussen<sup>2</sup>, Camilla O. Samuelsen<sup>2</sup>,  
Emmanouella Chatzidaki<sup>1</sup>, Vera Baraznenok<sup>1</sup>, Jenny Beve<sup>1</sup>, Peter Henriksen<sup>2</sup>,  
Claes M. Gustafsson<sup>1</sup> and Steen Holmberg<sup>2,\*</sup>

<sup>1</sup>Division of Metabolic Diseases, Karolinska Institutet, Novum, SE-141 86 Stockholm, Sweden and

<sup>2</sup>Department of Molecular Biology, Copenhagen Biocenter, University of Copenhagen, Ole Måloes Vej 5, DK-2200 Copenhagen N, Denmark

Received January 28, 2008; Revised and accepted February 5, 2008

## ABSTRACT

Mediator is an evolutionary conserved coregulator complex required for transcription of almost all RNA polymerase II-dependent genes. The *Schizosaccharomyces pombe* Mediator consists of two dissociable components—a core complex organized into a head and middle domain as well as the Cdk8 regulatory subcomplex. In this work we describe a functional characterization of the *S. pombe* Mediator. We report the identification of the *S. pombe* Med20 head subunit and the isolation of its alleles of the core head subunit encoding *med17<sup>+</sup>*. Biochemical analysis of *med8<sup>ts</sup>*, *med17<sup>ts</sup>*,  $\Delta med18$ ,  $\Delta med20$  and  $\Delta med27$  alleles revealed a stepwise head domain molecular architecture. Phenotypical analysis of Cdk8 and head module alleles including expression profiling classified the Mediator mutant alleles into one of two groups. Cdk8 module mutants flocculate due to overexpression of adhesive cell-surface proteins. Head domain-associated mutants display a hyphal growth phenotype due to defective expression of factors required for cell separation regulated by transcription factor Ace2. Comparison with *Saccharomyces cerevisiae* Mediator expression data reveals that these functionally distinct modules are conserved between *S. pombe* and *S. cerevisiae*.

## INTRODUCTION

The Mediator is a multiprotein coregulator complex that is required for the transcription of almost all RNA polymerase II (pol II)-dependent genes in fungi and metazoans (1). Mediator is thought to act as an interface between the general transcription machinery and sequence-specific transcriptional activators. A pure yeast *in vitro* transcription system consisting of pol II and all the general transcription factors (GTFs) cannot be stimulated by activators in the absence of Mediator (2,3).

Mediator was originally purified in *Saccharomyces cerevisiae* and has since then been isolated from several other eukaryotic species (1,4,5). These biochemical data revealed a core set of Mediator subunits that are conserved in most, if not all eukaryotes (6–8).

We have previously isolated and characterized the Mediator complex from *Schizosaccharomyces pombe* (6,9). The *S. pombe* Mediator exists in at least three states: a smaller core Mediator complex (S-Mediator) consisting of 15 subunits, a larger form (L-Mediator) consisting of core Mediator bound to a four-subunit module known as the Cdk8 module, and finally as a holoenzyme form with the core Mediator bound to pol II (9–11).

The Cdk8 module in both *S. cerevisiae* and *S. pombe* consists of four proteins: Med12 and Med13 as well as the cyclin-dependent kinase Cdk8 and its cyclin CycC (10,12). Both *S. cerevisiae* and *S. pombe* Cdk8 are able to phosphorylate the C-terminal domain of the largest subunit of pol II *in vitro*, which is thought to inhibit

\*To whom correspondence should be addressed. Tel: +45 35322119; Fax: +45 3532128; Email: gensteen@bio.ku.dk  
Correspondence may also be addressed to Tomas Linder. Tel: +1 415 476 3068; Fax: +1 415 514 9736; Email: tlinder@cmp.ucsf.edu  
Present address:

Tomas Linder, Department of Cellular and Molecular Pharmacology, University of California San Francisco, 1700 4th Street, PO Box 25430, Byers Hall 4308A, San Francisco, CA 94158-25430, USA

Nina N. Rasmussen, Evolva A/S, Bülowsvej 25, DK-1870 Frederiksberg C, Denmark

transcriptional initiation (10,13). Titration of the Cdk8 module-containing L-Mediator into an *in vitro* *S. pombe* transcription system has been shown to counteract the stimulatory effect of Mediator on basal transcription (14). Yet there is also evidence of a positive role for the Cdk8 module in activation (15,16).

Electron microscopy (EM) studies of single *S. cerevisiae* core Mediator particles identified three distinct domains that have been named head, middle and tail (17,18). A similar investigation showed that the *S. pombe* core Mediator also contained a head and a middle domain, but lacked a visible tail domain (11). In agreement with this, only one of the five *S. cerevisiae* tail subunits, Med15, is conserved in *S. pombe*. So far Med15 has not been identified as a stable component of *S. pombe* Mediator.

Based on work in *S. cerevisiae*, the *S. pombe* middle domain is suggested to consist of Med1, Med4, Med7, Med10, Med14, Med19, Med21 and Med31 (19–23). The architecture of the *S. cerevisiae* head domain has been extensively characterized (20–25). From these data, we predict that the *S. pombe* head domain consists of Med8, Med17, Med18 and Med22 as well as the proposed Med20 subunit, which has not been identified as a stable Mediator component prior to this work.

Here, we describe a structural and functional characterization of a representative set of subunits of the *S. pombe* Mediator. We identify the nonessential set of subunits in the head domain including a new subunit homologous to *S. cerevisiae* Med20. We report the isolation and characterization of conditional alleles of the essential head domain component Med17 and discuss its role in head domain architecture. Phenotypical analysis in combination with expression profiling of a representative set of Mediator mutant alleles allowed us to define two distinct functional classes of subunits within the *S. pombe* Mediator complex. Finally, the role of these separate classes of Mediator subunits in specific cellular pathways is discussed.

## MATERIAL AND METHODS

### *Schizosaccharomyces pombe* strains

All yeast strains used in this study are listed in Table 1. *Schizosaccharomyces pombe* cells were transformed by the lithium acetate procedure (26). Null mutants of *med15*<sup>+</sup>, *med18*<sup>+</sup> and *med20*<sup>+</sup> for expression profiling were generated using the kanMX selectable marker in the haploid *h*<sup>-</sup> strain MP9 as described (6) using the primers listed in Supplementary Table S1. The double null mutant of *med18*<sup>+</sup> and *med20*<sup>+</sup> was constructed by crossing and tetrad analysis of the diploid TP396/TP235. Null mutants of *med18*<sup>+</sup>, *med20*<sup>+</sup> and *med27*<sup>+</sup> for protein purification were generated with the *ura4*<sup>+</sup> gene as a selectable marker in an *Ura*<sup>-</sup> background. A plasmid containing the wild-type *ura4*<sup>+</sup> gene (GenBank accession number X13976), pURA4, was constructed by inserting it into HindIII-digested pBluescript II SK (Stratagene). Segments of 500-bp flanking the *med18*<sup>+</sup>, *med20*<sup>+</sup> and *med27*<sup>+</sup> genes were PCR amplified and inserted on either side of the *ura4*<sup>+</sup> marker to generate the plasmids pURA4-*spmed18*,

pURA4-*spmed20* and pURA4-*spmed27*, respectively. The knockout fragments were released from the respective plasmids by digesting with PvuII and transformed into the diploid strain TP219/TP220 carrying a Tandem Affinity Purification (TAP) tag on both copies of the *med7*<sup>+</sup> gene. The obtained *Ura*<sup>+</sup> diploids were sporulated and *Ura*<sup>+</sup>/G418-resistant spores were recovered, to generate strains TP416, TP417 and TP306, respectively.

### Isolation of *med17*<sup>ts</sup> mutants

A marker switch approach (27) was used for the construction of *med17*<sup>ts</sup> mutants. The *LEU2* gene was inserted in a PacI site at 159 bp 3' of *med17*<sup>+</sup> ORF in strain MP1 to generate TP384. The *med17*<sup>+</sup> gene from position 429 bp 5' to 212 bp 3' of the *med17*<sup>+</sup> ORF was cloned in pBluescript SK +/- and the 1.8-kb HindIII *ura4*<sup>+</sup> fragment of pREP42X (28,29) was inserted into the PacI site at 159 bp 3' of the *med17*<sup>+</sup> ORF to generate plasmid pTK1276. Mutagenesis of pTK1276 plasmid DNA was carried out with hydroxylamine (29) as follows: 10 µg of plasmid DNA was added to 500 µl ice-cold hydroxylamine solution (1 M H<sub>2</sub>NO-HCL, adjusted to pH 7 with NaOH) and incubated at 75°C for 90 min. Reactions were stopped by adding 200 mM NaCl, DNA was collected by EtOH precipitation and transformed in *Escherichia coli* strain DH5α. The *med17::ura4*<sup>+</sup> fragment was exerted from a pool of mutagenized pTK1276 DNA with ApaLI and PacI and transformed into strain TP384. *Ura*<sup>+</sup> transformants were selected on AA-Ura plates and replica-plated onto YES plates. After 3 days of incubation at 37°C, candidate colonies of temperature-sensitive (ts) mutants were isolated and tested for loss of the *LEU2* gene on AA-Leu plates. Screening of 10 000 yeast transformants for a ts phenotype at 37°C yielded four independent mutant strains with a ts phenotype at 37°C on YES plates.

### Construction of the *med17Δ50* allele

One hundred and fifty nucleotides from position 1601–1751 of the *med17*<sup>+</sup> ORF was deleted from plasmid pTK1276 introducing a NheI site 3' of the stop codon in the process to generate plasmid pTK1439. The *med17Δ50::ura4*<sup>+</sup> sequence was exerted from pTK1439 with ApaLI and PacI and transformed into diploid strain TP384/MP2. *Ura*<sup>+</sup> transformants were selected on AA-Ura plates and sporulated on MSA plates. After dissection *Ura*<sup>+</sup>/Leu<sup>-</sup> spores were tested for a ts phenotype at 37°C and an *ura4*<sup>+</sup> *leu2*<sup>-</sup> *med17Δ50* spore called TP390 isolated. The *ura4*<sup>+</sup> gene was removed from the *med17Δ50* strain TP390 by transforming with an 812-bp fragment spanning the *ura4*<sup>+</sup> gene but not running into the *med17*<sup>+</sup> ORF followed by selection on 5-FOA plates giving strain TP392.

### TAP-tagging of *med7*<sup>+</sup> in strain TP390 (*med17Δ50*) and strain MP10 (*sep15-598/med8*<sup>ts</sup>)

The C-terminal part of the *med7*<sup>+</sup> gene fused to a TAP-tag was exerted from plasmid pFA6a-kanMX6-CTAP2-*spmed7* (10) with AvrII and EcoRV and transformed into the *med17Δ50* strain TP392 and *sep15-598/med8*<sup>ts</sup> strain

**Table 1.** Yeast strains used in this study

Strain	Genotype	Parent strain(s)	Source
<i>S. pombe</i>			
MP1	<i>h</i> <sup>+</sup> <i>ade6-M210 his7-336 leu1-32 ura4-D18</i>	ID CHP429	(6)
MP2	<i>h</i> <sup>-</sup> <i>ade6-M216 his7-336 leu1-32 ura4-D18</i>	ID CHP428	(6)
MP9	<i>h</i> <sup>-</sup>	L972	M. Sipiczki
MP10	<i>h</i> <sup>90</sup> <i>sep15-598 his3</i>	2-506	(44)
MP12	<i>h</i> <sup>-</sup> <i>ade6-M210</i>	IH105	Ian Hagan
MP13	<i>h</i> <sup>+</sup> <i>ade6-M216</i>	IH107	Ian Hagan
TP21	<i>h</i> <sup>-</sup> <i>Δmed1::kanMX4</i>	MP9	This study
TP26	<i>h</i> <sup>-</sup> <i>Δmed18::kanMX4</i>	MP9	This study
TP27	<i>h</i> <sup>-</sup> <i>Δmed12::kanMX4</i>	MP9	This study
TP28	<i>h</i> <sup>-</sup> <i>Δmed12::kanMX4</i>	MP9	(10)
TP42	<i>h</i> <sup>+</sup> <i>ade6-M210 med7</i> <sup>+</sup> <i>::TAP-kanMX6</i>	MP12/MP13 <sup>a</sup>	This study
TP47	<i>h</i> <sup>-</sup> <i>ade6-M216 med8</i> <sup>+</sup> <i>::TAP-kanMX6</i>	MP12/MP13 <sup>a</sup>	This study
TP126	<i>h</i> <sup>-</sup> <i>Δmed18::kanMX4</i>	MP9	This study
TP130	<i>h</i> <sup>-</sup> <i>Δmed15::kanMX4</i>	MP9	This study
TP192	<i>h</i> <sup>-</sup> <i>cdk8-D158A (dead-kinase mutant) ura4-D18 leu1-32</i>		(11)
TP207	<i>h</i> <sup>+</sup> <i>cdk8-D158A (dead-kinase mutant)</i>	TP192/MP13 <sup>a</sup>	This study
TP216	<i>h</i> <sup>+</sup> <i>ade6-M216 ura4-D18 med7</i> <sup>+</sup> <i>::TAP-kanMX6</i>	TP42/MP2 <sup>b</sup>	This study
TP234	<i>h</i> <sup>-</sup> <i>Δmed20::kanMX4</i>	MP9	This study
TP235	<i>h</i> <sup>+</sup> <i>Δmed20::kanMX4 ade6-M210</i>	MP12/MP13 <sup>a</sup>	This study
TP274	<i>h</i> <sup>-</sup> <i>cdk8-D158A (dead-kinase mutant)</i>	TP207/MP9 <sup>b</sup>	This study
TP306	<i>h</i> <sup>+</sup> <i>ade6-M216 ura4-D18 med7</i> <sup>+</sup> <i>::TAP-kanMX6 Δmed27::ura4</i> <sup>+</sup>	TP219/TP220 <sup>a</sup>	This study
TP308	<i>h</i> <sup>90</sup> <i>sep15-598 his3 med7</i> <sup>+</sup> <i>::TAP-kanMX6</i>	2-506	This study
TP315	<i>h</i> <sup>+</sup> <i>ade6-M210 his7-336 leu1-32 ura4-D18 med7</i> <sup>+</sup> <i>::TAP-kanMX med17Δ50</i>	TP392	This study
TP316	<i>h</i> <sup>-</sup> <i>Δmed31::kanMX4</i>	MP9	This study
TP384	<i>h</i> <sup>+</sup> <i>ade6-M210 his7-336 leu1-32 ura4-D18 med17</i> <sup>+</sup> <i>::LEU2</i>	MP1	This study
TP390	<i>h</i> <sup>+</sup> <i>ade6-M210 his7-336 leu1-32 ura4-D18 med17Δ50::ura4</i> <sup>+</sup>	TP384/MP2 <sup>a</sup>	This study
TP392	<i>h</i> <sup>+</sup> <i>ade6-M210 his7-336 leu1-32 ura4-D18 med17Δ50</i>	TP390	This study
TP396	<i>h</i> <sup>-</sup> <i>Δmed18::hph (hph: Hygromycin B Phosphotransferase)</i>	TP26	This study
TP405	<i>h</i> <i>Δmed18::hph Δmed20::kanMX4</i>	TP396/TP235 <sup>b</sup>	This study
TP416	<i>h</i> <sup>+</sup> <i>ade6-M216 ura4-D18 med7</i> <sup>+</sup> <i>::TAP-kanMX6 Δmed18::ura4</i> <sup>+</sup>	TP216	This study
TP417	<i>h</i> <sup>+</sup> <i>ade6-M216 ura4-D18 med7</i> <sup>+</sup> <i>::TAP-kanMX6 Δmed20::ura4</i> <sup>+</sup>	TP216	This study
ND064	<i>h</i> <sup>-</sup> <i>Δace2::kanMX4</i>		(68)
ND102	<i>h</i> <sup>-</sup> <i>Δsep1::kanMX4</i>		(68)
<i>S. cerevisiae</i>			
BY4741	<i>MAT a his3Δ1 leu2Δ0 met15Δ0 ura3Δ0</i>		EUROSCARF
Y01742	<i>MAT a his3Δ1 leu2Δ0 met15Δ0 ura3Δ0 Δmed15::kanMX</i>	BY4741	EUROSCARF
Y04393	<i>MAT a his3Δ1 leu2Δ0 met15Δ0 ura3Δ0 Δmed3::kanMX</i>	BY4741	EUROSCARF
Y04494	<i>MAT a his3Δ1 leu2Δ0 met15Δ0 ura3Δ0 Δmed31::kanMX</i>	BY4741	EUROSCARF
Y04734	<i>MAT a his3Δ1 leu2Δ0 met15Δ0 ura3Δ0 Δmed18::kanMX</i>	BY4741	EUROSCARF
Y05351	<i>MAT a his3Δ1 leu2Δ0 met15Δ0 ura3Δ0 Δcycc::kanMX</i>	BY4741	EUROSCARF
Y05799	<i>MAT a his3Δ1 leu2Δ0 met15Δ0 ura3Δ0 Δmed12::kanMX</i>	BY4741	EUROSCARF
Y06611	<i>MAT a his3Δ1 leu2Δ0 met15Δ0 ura3Δ Δmed20::kanMX</i>	BY4741	EUROSCARF
Y13701	<i>MAT a his3Δ1 leu2Δ0 met15Δ0 ura3Δ Δmed2::kanMX</i>	BY4741	EUROSCARF
TAP-Med8	<i>MAT a pep4::HIS3/prb1::LEU2 prc1::HISG can1 ade2 trp1 ura3 his3 leu2-3, 112 MED8::TAP-klTRP1</i>	CB010	(12)
CGC129	<i>MAT a pep4::HIS3/prb1::LEU2 prc1::HISG can1 ade2 trp1 ura3 his3 leu2-3, 112 MED8::TAP-klTRP1 Δmed18::kanMX6</i>	TAP-Med8	This study
CGC130	<i>MAT a pep4::HIS3/prb1::LEU2 prc1::HISG can1 ade2 trp1 ura3 his3 leu2-3, 112 MED8::TAP-klTRP1 Δmed20::kanMX6</i>	TAP-Med8	This study

<sup>a</sup>Spore obtained after transformation of the diploid and subsequent sporulation of the diploid.

<sup>b</sup>Spore obtained after mating and sporulation of the diploid.

MP10 giving strains TP315 and TP308, respectively. Correct integration of constructs in the genome was verified by PCR analysis. The MP10 strain was a kind gift from M. Sipiczki (University of Debrecen, Hungary). In all cases, tetrad analysis and/or Southern blot analysis were/was applied to demonstrate that only one copy of the construct had integrated in the genome.

### *Saccharomyces cerevisiae* strains

All *S. cerevisiae* deletion strains were purchased from Euroscarf. Deletion cassettes of the *MED20* and *MED18*

genes were generated by amplifying the kanMX cassette from Euroscarf deletion strains BY0661 (*Δmed20*) and BY04734 (*Δmed18*) with 500-bp flanking sequence on either side of the kanMX marker. *Saccharomyces cerevisiae* TAP-MED8 cells were transformed with the amplified deletion cassettes using the lithium acetate procedure. Correct genomic integration was assayed by PCR using primers positioned at the very 5' end of either the upstream or coding region and conversely outside the 3' flanking regions of the transformation constructs. The TAP-MED8 strain (12) was a kind gift from Roger Kornberg (Stanford University, CA, USA).

### Protein purification

Cells were grown at 30°C unless otherwise specified. *Saccharomyces cerevisiae* cells were grown in YPD medium (10 g/l yeast extract, 20 g/l peptone, 20 g/l glucose) to OD<sub>600</sub> 3.5–4.0, and *S. pombe* cells were cultured to OD<sub>600</sub> 2.0–2.5 in yeast extract supplement (YES) medium (5 g/l yeast extract, 2 g/l casamino acids, 20 g/l glucose) supplemented with 0.2 g/l adenine. For preparation of whole-cell extract, we collected yeast cells from a 10 l culture by centrifugation (Beckman Instruments JLA-10 500 rotor, 9500 r.p.m., 10 min, 4°C), which were washed once with ice-cold water and suspended in 0.5 ml of 3 × lysis buffer (200 mM HEPES-KOH, pH 7.8, 15 mM KCl, 1.5 mM MgCl<sub>2</sub>, 0.5 mM EDTA, 15% glycerol, 0.5 mM dithiothreitol and protease inhibitors) per gram of cell pellet. For all purifications, we used a 100 × stock of protease inhibitors containing 100 mM phenylmethylsulfonyl fluoride, 200 mM pepstatin, 60 mM leupeptin and 200 mM benzamidine in 95% ethanol. Cells were lysed by bead beating (Bead-Beater, Stratech, London, UK) for 25 cycles, with each cycle consisting of 30 s of beating and 90 s of rest. We cleared the supernatant by centrifugation (Beckman Instruments JLA-10 500 rotor at 9500 r.p.m., for 10 min, at 4°C), added 1/9 vol of 2 M KCl and stirred for 15 min. Polyethyleneimine was added to a final concentration of 0.02% followed by 15 min of stirring. Insoluble material was removed by ultracentrifugation (Beckman Instruments Ti45 rotor, 42 000 r.p.m., 30 min, 4°C). Mediator was purified according to the original TAP-tag purification protocol (30,31) with the following modifications. Nine hundred microliters of IgG–Sepharose (GE Healthcare) was added to 200 ml of extract and incubated for 2 h at 4°C. The IgG–Sepharose was collected by centrifugation (Beckman Instruments JA-17 rotor, 800 r.p.m., 1 min, 4°C), loaded onto a Poly-Prep column (Bio-Rad) and washed with 100 ml of IgG wash buffer (20 mM HEPES-NaOH, pH 7.5, 150 mM NaCl, 0.1% IGEPAL CA-630). Mediator was eluted in two steps: first, by incubation for 2 h at 16°C with 200 U of tobacco etch virus (TEV) NIa protease (Invitrogen) in 2 ml of TEV buffer (10 mM HEPES-NaOH, pH 7.5, 150 mM NaCl, 0.5 mM EDTA, 0.1% IGEPAL CA-630, 1 mM dithiothreitol), designated IgG eluate 1, and second, by elution of the IgG–Sepharose by incubation with 8 M urea, 100 mM NaH<sub>2</sub>PO<sub>4</sub>, 10 mM Tris–HCl, pH 7.7, for 5 min at room temperature, designated IgG eluate 2. For further purification of *S. pombe* Mediator, 500 µl of IgG eluate 1 was loaded onto a 1-ml heparin HiTrap column (GE Healthcare). The column was washed with 5 ml of buffer A-0.1 (20 mM HEPES-NaOH, pH 7.5, 10% glycerol, 0.5 mM EDTA, 1 mM dithiothreitol, protease inhibitors and the molarity of sodium chloride indicated after the hyphen) and then developed with a linear gradient (12 ml) of A-0.1 to A-1.2.

### Immunoblotting and production of antibodies

The full-length *S. pombe med20*<sup>+</sup> coding region (GenBank accession NM\_001019159) was inserted into the expression plasmid pGEX3X (GE Healthcare). The GST-Med20 fusion-protein was overexpressed in *E. coli* BL21 (DE3)

pLysS cells (Stratagene) and subsequently purified using glutathione–Sepharose 4B (GE Healthcare) according to the recommendations of the manufacturer. The purified GST-Med20 protein was used to immunize rabbits. The antisera used in this study were taken 10 days after the second booster injection (AgriSera, Vännäs, Sweden). Antibodies specific for *S. pombe* Mediator subunits Med17, Med18, Med27 and Med31 have been described previously (6,9,32). Antibodies specific for *S. pombe* CycC will be described in a parallel publication (Baraznenok, V. and Gustafsson, C.M., submitted for publication). *Schizosaccharomyces pombe* TAP-Med7 was detected with the soluble peroxidase anti-peroxidase complex (Sigma). Antibodies specific for *S. cerevisiae* Mediator subunits Med1, Med2, Med8 and Med11 were kind gifts from Stefan Björklund (Umeå University, Sweden). Antibodies against *S. cerevisiae* Med18 and Med20 were kind gifts from R.A. Young (Whitehead Institute for Biomedical Research, Cambridge, MA, USA).

### Affymetrix GeneChip probe array hybridization

*Schizosaccharomyces pombe* strains were grown in EMM medium at 30°C until  $5 \times 10^6$  to  $1 \times 10^7$  cells/ml. Heat-stressed wild-type and *med17Δ50* cells were cultured in EMM at 30°C until  $5 \times 10^6$  to  $1 \times 10^7$  cells/ml, spun down briefly and then resuspended in media pre-warmed to 37°C. Cells were harvested after 2 h of incubation at 37°C. Total yeast RNA was isolated using a hot acid phenol extraction protocol (33). Labeling and array hybridization to Affymetrix Yeast Genome 2.0 arrays were performed at the Karolinska Institute Affymetrix core facility (Huddinge, Sweden). Labeling and hybridization protocols are described in the Affymetrix users' manual (34). Washing and staining of arrays were performed using the GeneChip Fluidics Station 450. Arrays were scanned with the Affymetrix GeneArray scanner 3000 7G. Acquisition and quantification of array images as well as primary data analysis including normalization was performed using Affymetrix GeneChip Operating Software (GCOS). Data were processed with the MAS5 algorithm (scaling: all probe sets with target signal 100, normalization: user defined with normalization value 1). The expression profiling was done on two sets of samples. The first set contained transcript level data from three wild-type (MP9) cultures and three cultures of each of the *cdk8*<sup>mut</sup>, *Δmed12*, *Δmed15*, *Δmed18* and *Δmed20* strains. The second set contained transcript level data from two *med17Δ50* mutant cultures and two corresponding wild-type (MP1) cultures. To rule out the possibility of global changes to the transcriptome in the Mediator mutants, all datasets were normalized to an internal housekeeping control mRNA. Through quantitative real-time PCR (see below) we established that the *atp1*<sup>+</sup> gene displayed <1.5-fold change in all mutants when normalized to 28 S rRNA levels and was therefore chosen as the internal mRNA control. Within each set of samples the transcript signal intensities was compared to all the corresponding wild-type baseline controls, generating a total of nine comparisons for each mutant in the first series. The Affymetrix change-call algorithm designated every transcript in each

individual comparison as increased, decreased or invariant ( $P$ -value threshold 0.0025) with reference to the wild-type baseline intensity. An average ratio change was calculated for each transcript in each strain by first adjusting the ratio change to one of all comparisons designated invariant and then calculating the geometric mean for the total number of comparisons. The normalized and filtered dataset is available as Supplementary Data in the online version of this article.

### Clustering and statistical analysis of expression data

Hierarchical clustering was carried out with the TIGR Multiexperiment Viewer version 3.0.3 (35). Ortholog tables for *S. pombe* and *S. cerevisiae* were kindly provided by Valerie Wood at the Wellcome Trust Sanger Institute *S. pombe* Genome Project. Genomic coordinates for *S. pombe* genes were retrieved from the *S. pombe* Genome Database. Expression data for the *S. pombe med8<sup>ts</sup>/sep15-598* and *med31<sup>ts</sup>/sep10-412* mutants (36) (ArrayExpress accession E-MEXP-193) as well as the *Aace2* and *Asep1* mutants (37) (ArrayExpress accession E-MEXP-62) were downloaded from the Bähler lab homepage ([http://www.sanger.ac.uk/PostGenomics/S\\_pombe/projects/](http://www.sanger.ac.uk/PostGenomics/S_pombe/projects/)). Missing values were set to ratio 1. The list of *S. pombe* core environmental stress response (CESR) genes is from ref. 38.

### Quantitative real-time PCR

Total RNA was isolated as described above. RNA quality and concentration was determined using a BioAnalyser 2100 (Agilent). cDNA was synthesized with the AMV 1st Strand Synthesis Kit (Roche) using random hexamers. Relative quantification of cDNA was carried out in triplicate on a LightCycler 2.0 (Roche) using SYBR green technology and the FastStart DNA Master SYBR Green 1 mix (Roche). Standard curves were generated by at least four 5-fold serial dilutions of a single control sample and values within the linear exponential phase were used to calculate relative concentrations after normalization. Primers used for quantitative PCR are listed in Supplementary Table S2.

### Northern blotting

Northern blotting was done as previously described (39) using 2  $\mu$ g of heat-denatured total RNA (65°C for 3 min) in each lane. The <sup>32</sup>P-labeled poly(dT) probe was obtained by reverse transcription: a 10  $\mu$ l reaction containing 50 ng poly(rA), 100 pmol oligo(dT)<sub>18</sub> primer, 1  $\mu$ l 10  $\times$  M-MuLV reverse transcriptase reaction buffer [50 mM Tris-HCl (pH 8,3), 75 mM KCl, 3 mM MgCl<sub>2</sub>, 10 mM DTT], 100 pmol dTTP, 10  $\mu$ Ci [ $\alpha$ -<sup>32</sup>P] dTTP (400 Ci/mmol), 100 U Moloney murine leukemia virus (M-MuLV) reverse transcriptase (NEBiolabs) was carried out at 37°C for 1 h. The poly(rA) template was removed by RNase H treatment where after RNase H was heat inactivated.

## RESULTS

### Biochemical characterization of the *S. pombe* Mediator head domain

Mass spectrometric analysis of partially purified *S. pombe* Mediator identified the hypothetical protein SPAC17G8.05 (GenBank accession NP\_593728) as a potential Mediator subunit with an apparent mass of around 20 kDa (data not shown). SPAC17G8.05 has previously been predicted to be the *S. pombe* homolog of *S. cerevisiae* and mammalian Med20 (7). To demonstrate its stable Mediator association, *S. pombe* Mediator was purified with TAP-tag on the Med8 subunit and resolved by Heparin–Sephrose chromatography. Western analysis showed co-elution of Med20 with Med17 and Med27 (Figure 1A). Thus, Med20 is a stable subunit of *S. pombe* Mediator.

In *S. cerevisiae*, Med20 and Med18 form a distinct submodule within the head domain (24,25,40). Med20 is completely lost from *S. cerevisiae* Mediator isolated from a  $\Delta$ *med18* strain (Figure 1B, right lane). However, we could still detect reduced amounts of Med18 associated with Mediator isolated from a  $\Delta$ *med20* strain (Figure 1B, middle lane).

To establish whether the *S. pombe* head domain is organized as that of *S. cerevisiae* diploid strains heterozygous for either  $\Delta$ *med18* or  $\Delta$ *med20* were made. After tetrad analysis, viability segregated 4:0 showing that both *med18*<sup>+</sup> and *med20*<sup>+</sup> are nonessential genes in *S. pombe* like their *S. cerevisiae* homologs. Both  $\Delta$ *med18* and  $\Delta$ *med20* *S. pombe* cells have a slow growth phenotype and fail to sporulate (data not shown) (41). We purified Mediator from strains lacking either *med18*<sup>+</sup> or *med20*<sup>+</sup>, respectively, utilizing a TAP-tag on Med7 (Figure 1C). In agreement with our observations in budding yeast,  $\Delta$ *med20* *S. pombe* Mediator contained reduced amounts of the Med18 subunit, whereas mutant  $\Delta$ *med18* Mediator completely lacked Med20 after purification over IgG–Sephrose. In addition, both the  $\Delta$ *med18* and  $\Delta$ *med20* mutant Mediator lacked the Med27 subunit. No homolog of Med27 has been identified in the *S. cerevisiae* Mediator. Cells lacking *med27*<sup>+</sup> (systematic name SPAC17C9.05c) are viable without any apparent phenotype at 30°C (data not shown) (6). Mediator purified from  $\Delta$ *med27* TAP-*med7*<sup>+</sup> cells still contained both Med18 and Med20 (Figure 1D, middle lane) consistent with the wild-type growth phenotype at 30°C of  $\Delta$ *med27* cells. This suggests that Med27 is located proximally to the Med18/Med20 dimer on the periphery of the head domain.

A *ts* allele of the essential head domain subunit Med8 called *sep15-598* (or *med8<sup>ts</sup>* for clarity) has been isolated (42–44). *Schizosaccharomyces pombe* cells carrying the *med8<sup>ts</sup>* allele display a similar growth phenotype as  $\Delta$ *med18* cells suggesting that this allele could affect subunit interactions within the head domain (42). Western blot analysis revealed that Mediator purified from a *med8<sup>ts</sup>* TAP-*med7*<sup>+</sup> strain had lost Med18, Med20 and Med27 (Figure 1D, right lane). Furthermore, Med8 interacts with Med20 in a yeast two-hybrid interaction analysis (data not shown). Thus, our observations suggest a step-wise structural organization of the nonessential *S. pombe*

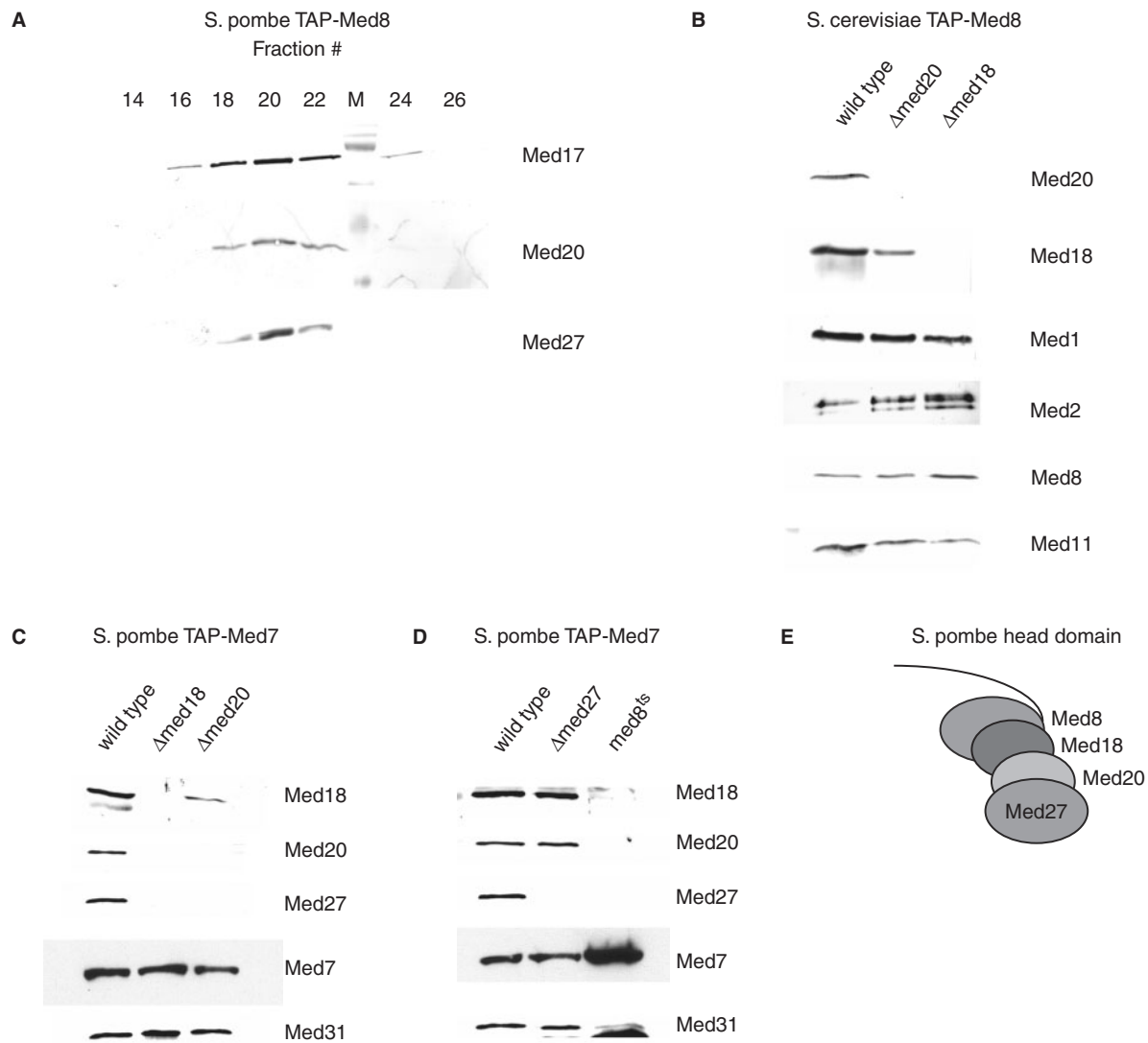


**Figure 1.** Structural organization of the *S. pombe* Mediator head domain. (A) *Schizosaccharomyces pombe* TAP-Med8 Mediator was eluted from IgG-Sepharose by TEV cleavage and further resolved over Heparin-Sepharose as described in 'Material and methods' section. Western analysis of different fractions. (B) Western analysis of *S. cerevisiae* Mediator purified through a TAP-tag on the Med8 subunit from wild-type,  $\Delta med20$  and  $\Delta med18$  cells. (C) Western analysis of *S. pombe* Mediator purified through a TAP-tag on the Med7 subunit from wild-type,  $\Delta med18$  and  $\Delta med20$  cells. (D) Western analysis of *S. pombe* Mediator purified through a TAP-tag on the Med7 subunit from wild-type,  $\Delta med27$  and  $med8^{ts}/sep15-598$  cells. (E) Proposed subunit organization of the *S. pombe* head domain based on the results in (C) and (D).

head domain subunits where Med27 is found on the very exterior connected to Med20, which in turn contacts Med18 that binds Med8 (Figure 1E). This model is in agreement with recent structural data of a Med8-Med18-Med20 trimer in *S. cerevisiae* (40).

#### Isolation and characterization of *S. pombe med17* ts alleles

The *S. cerevisiae* Med17 subunit is located in the head domain and essential for cell viability (20,24,45) reflecting its importance as a scaffold for the remaining head domain subunits (22,25). The ts allele of *S. cerevisiae* MED17 termed *srb4-138* was instrumental in demonstrating the universal requirement for Mediator in pol II-dependent transcription *in vivo* (45,46). The *med17*<sup>+</sup> gene is also

essential in *S. pombe* (6). We constructed a conditional *med17* allele in *S. pombe* to understand Mediator function in fission yeast. We employed a marker switch approach (27) to establish a ts allele by targeted hydroxylamine mutagenesis at the *med17*<sup>+</sup> locus and isolated four independent mutant strains with a ts phenotype at 37°C on YES plates. All four *med17* mutants had acquired base changes in the C-terminal part of the *med17*<sup>+</sup> coding sequence resulting in premature stop codons within the last 50 C-terminal amino acids of the Med17 protein. We considered the possibility that low levels of read-through of the premature stop codon could still produce full-length Med17 protein and that a *de facto* C-terminal truncation would be lethal. Thus, we constructed a strain lacking the last 50 C-terminal amino acids and termed this *med17*

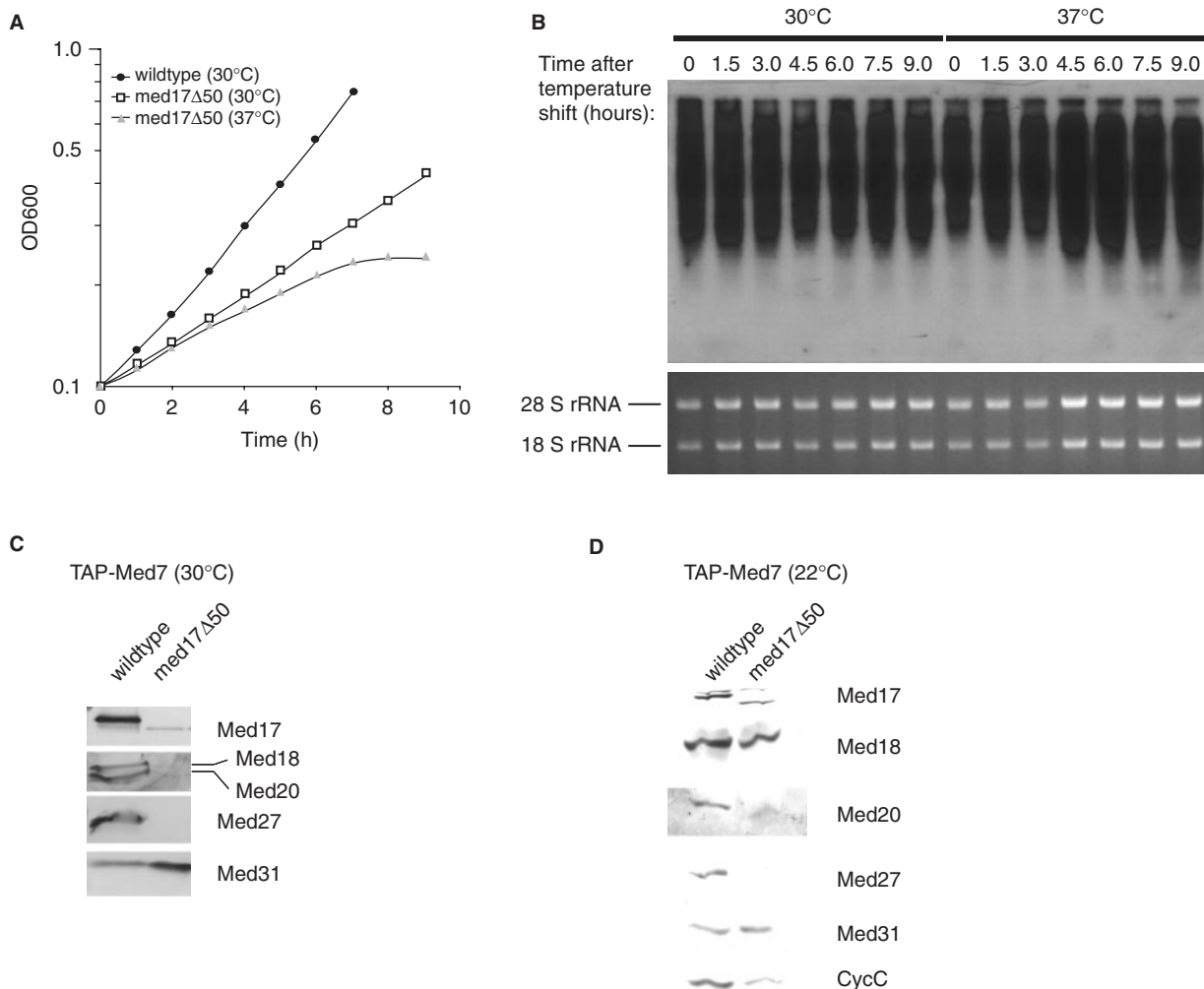


**Figure 2.** Isolation and characterization of temperature-sensitive alleles of the *S. pombe med17<sup>+</sup>* gene. **(A)** *med17Δ50* cells and wild type (MPI) were grown to OD<sub>600</sub> = 0.1 (10<sup>6</sup> cells/ml) in YES medium at 30°C. Cultures were then divided in two, spun down and resuspended in medium preheated to either 30°C or 37°C. Cell density was continually measured until growth of the *med17Δ50* culture at 37°C had ceased. Due to septation defects in the *med17Δ50* cells, samples were sonicated briefly prior to absorbance measurement. **(B)** Northern blot analysis of global mRNA levels in *med17Δ50* cells following resuspension in medium preheated at either 30°C or 37°C. The upper panel shows a membrane probed with radioactively labeled poly-T as described in 'Material and Methods' section. Lower panel indicates rRNA loading control as observed in the ethidium bromide-stained agarose gel. **(C)** Western analysis of Tap-purified *S. pombe* Mediator from *med17Δ50 TAP-med7<sup>+</sup>* cells grown at 30°C. **(D)** The same purification as in (C) but cells were cultured at 22°C.

allele *med17Δ50* allele, which has a ts phenotype indistinguishable from the four previously isolated *med17<sup>ts</sup>* alleles.

*Saccharomyces cerevisiae* cells with the *srb4-138* allele immediately stop growing after a shift to 37°C (45). *Schizosaccharomyces pombe med17Δ50* cells displayed a slightly more gradual response when heat stressed. After shifting a mid log culture of *S. pombe med17Δ50* cells growing at 30°C to 37°C an initial decrease of growth rate after 2.5 h was observed with growth ceasing altogether after 7.5 h (Figure 2A). The same pattern was obtained with the isolated *med17<sup>ts</sup>* alleles (data not shown). As the *S. pombe med17Δ50* allele appeared subtly different from the *S. cerevisiae srb4-138* allele, we isolated total RNA from *med17Δ50* cells and wild-type controls cultured at 30°C as well as 2 h after a shift to 37°C. In *S. cerevisiae*

*srb4-138* cells, transcription ceases abruptly with most mRNA transcripts gone after 1 h (45). In contrast, northern blot analysis of heat-shocked *S. pombe med17Δ50* cells show no detectable decrease in mRNA levels even after 9 h at 37°C (Figure 2B).

Mediator was purified from *med17Δ50 TAP-med7<sup>+</sup>* strain grown at 30°C in order to characterize its subunit composition. Western blotting of the TEV eluate revealed that the head module proteins Med17 and Med27 were completely lost while the amounts of Med18 and Med20 were severely reduced (Figure 2C). This drastic destabilization of *S. pombe med17Δ50* Mediator was reminiscent of *S. cerevisiae srb4-138* Mediator, which fractures at the head/middle domain boundary irrespective of growth temperature (19). We repeated the purification, culturing the *med17Δ50* cells at 22°C and in this case Med17 was

present in the *med17Δ50* Mediator (Figure 2D). The head module subunit Med18 was still present whereas both Med20 and Med27 were lost from the mutant complex. This suggested that Med17 could be interacting with Med20 and Med27 independently of Med18. In support of this notion, yeast two-hybrid interaction analysis revealed that Med17 has physical contacts with Med20 and Med27 (data not shown). We have no two-hybrid data regarding interactions between Med17 and Med18. Direct interactions between Med17 and Med20 have also been reported previously in *S. cerevisiae* Mediator (22,24). Thus, we suggest the structural organization of the *S. pombe* head domain subunits depicted in Figure 1E with Med27 situated on the exterior connected to Med20, which contacts Med18 that ultimately binds Med8. Med17 could serve as a scaffold interacting with Med8, Med20 and Med27.

### Phenotypical classification of head and Cdk8 module Mediator mutant alleles

To discern functional subdivisions among Mediator subunits, we investigated the phenotypes of null alleles of *med1*<sup>+</sup>, *med12*<sup>+</sup>, *med18*<sup>+</sup>, *med20*<sup>+</sup>, *med27*<sup>+</sup>, *med31*<sup>+</sup> as well as the SPBC146.01 gene encoding the proposed *MED15* homolog. Deletion of *med15*<sup>+</sup> in a diploid followed by tetrad analysis showed that *med15*<sup>+</sup> is nonessential in *S. pombe*. We included the dead-kinase mutant allele of *cdk8*<sup>+</sup> called *cdk8<sup>mut</sup>* (11) as well as *med8<sup>ts</sup>* (42) and *med17Δ50*. All mutants displayed one of two specific cellular morphologies—flocculation or hyphal growth (Figure 3A). Flocculation signifies the aggregation of yeast cells into larger clumps (47) and has previously been observed in *Δcdk8*, *Δmed12* and *Δmed13* cells (10,48). Hyphal growth occurs when cells are unable to cleave the primary septum that separates two daughter cells following medial septation at the end of mitosis (49). This phenotype had previously been observed in ts alleles of *med8*<sup>+</sup>, *med18*<sup>+</sup> and *med31*<sup>+</sup> (41,44). The cellular morphology of the head domain mutants *med17Δ50*, *Δmed18* and *Δmed20* corresponded to the hyphal growth seen for the *med8*<sup>+</sup> ts allele *sep15-598*. The *Δmed27* mutant did not have a visible phenotype at 30°C, but showed some septation defects at 37°C (Figure 3A). A complete deletion of middle domain subunit *med31*<sup>+</sup> also displayed a hyphal growth phenotype in agreement with previous report (41). Interestingly, the *Δmed15* mutant also showed this phenotype. We included the two null mutants of G2/M transcription factors Ace2 and Sep1 for comparison, both of which display a severe septation defect (50–52). The Cdk8 module mutants flocculated, but showed no septation defects. Mutants lacking the *med1*<sup>+</sup> gene did not have a visible phenotype at 30°C, but flocculated at 37°C. In summary, we observed a clear distinction in cellular morphology between Cdk8 module mutants (and the associated middle domain subunit Med1) and those of the head domain as well as of middle domain subunit Med31 and the potential Mediator subunit Med15.

We observed varying degrees of severity in the hyphal growth phenotype in the head domain mutants, *Δmed15*

and *Δmed31*. A spot assay was carried out to further discern the magnitude of growth inhibition in the septating mutants (Figure 3B). We included *Δace2* and *Δsep1* for comparison. Cells were challenged with elevated temperatures (37°C), high salt (750 mM KCl) and 1% formamide, respectively. The *Δmed27* mutant appeared nearly indistinguishable from wild-type cells at all conditions tested. The *Δmed20* mutant was slightly more sensitive than wild type at high salt, but was very sensitive to heat and formamide. The remaining head domain mutants *med8<sup>ts</sup>*, *med17Δ50*, *Δmed18* as well as a *Δmed18 Δmed20* double mutant grow very poorly at all conditions tested. Thus, in these assays *Δmed18* is epistatic to *Δmed20*. Equal degree of sensitivity was observed for the *Δmed31* and *Δmed15* mutants. The two mutants *Δace2* and *Δsep1* were indistinguishable from wild type indicating that it was not the hyphal growth defect in itself that caused slow growth and stress sensitivity in the Mediator mutants. The Cdk8 module mutants were indistinguishable from wild type under all conditions tested (data not shown).

### Expression profiling of Mediator mutants

We asked whether the distinct morphological phenotypes of Mediator mutants reflected distinct effects on global gene transcription. Hence, we performed expression profiling on six mutant alleles that we considered a representative cross section of the *S. pombe* Mediator. Global expression profiles of mutant alleles in conjunction with hierarchical clustering analysis can be used in an analogous way to phenotypes as a way to discern functional relationships (53).

We made two sets of comparisons. The first set of comparisons consisted of three independent cultures of each of the mutant strains *cdk8<sup>mut</sup>* (TP274), *Δmed12* (TP27), *Δmed15* (TP130), *Δmed18* (TP126) and *Δmed20* (TP234) as well as a wild-type (MP9) control. The second set of comparisons consisted of two independent *med17Δ50* cultures (TP392) with two wild-type (MP1) controls. We employed the Affymetrix platform and the number of genes changing in each mutant by a defined ratio threshold is shown in Figure 4B.

We performed hierarchical clustering (54) on all genes changing 2-fold or more in the mutant datasets. The robustness of the clustering was tested by bootstrap analysis of 10 000 replicates with re-sampling of genes. The Cdk8 module mutants were clearly separated from the head domain subunits Med17, Med18 and Med20 (Figure 4A) as illustrated by the 100% bootstrap support of the Cdk8 module clade. The *Δmed15* mutant clustered within the head domain clade (Figure 4A), which is in agreement with previous results from *S. cerevisiae* Mediator (53). The genes that did change 2-fold or more belonged to diverse set of functional groups with no particular group of genes dominating any one expression profile—a reflection of the central role of Mediator in all pol II-dependent transcription. In addition, despite the significant correlation between expression profiles shown Figure 4A, each profile contained a set of genes particular



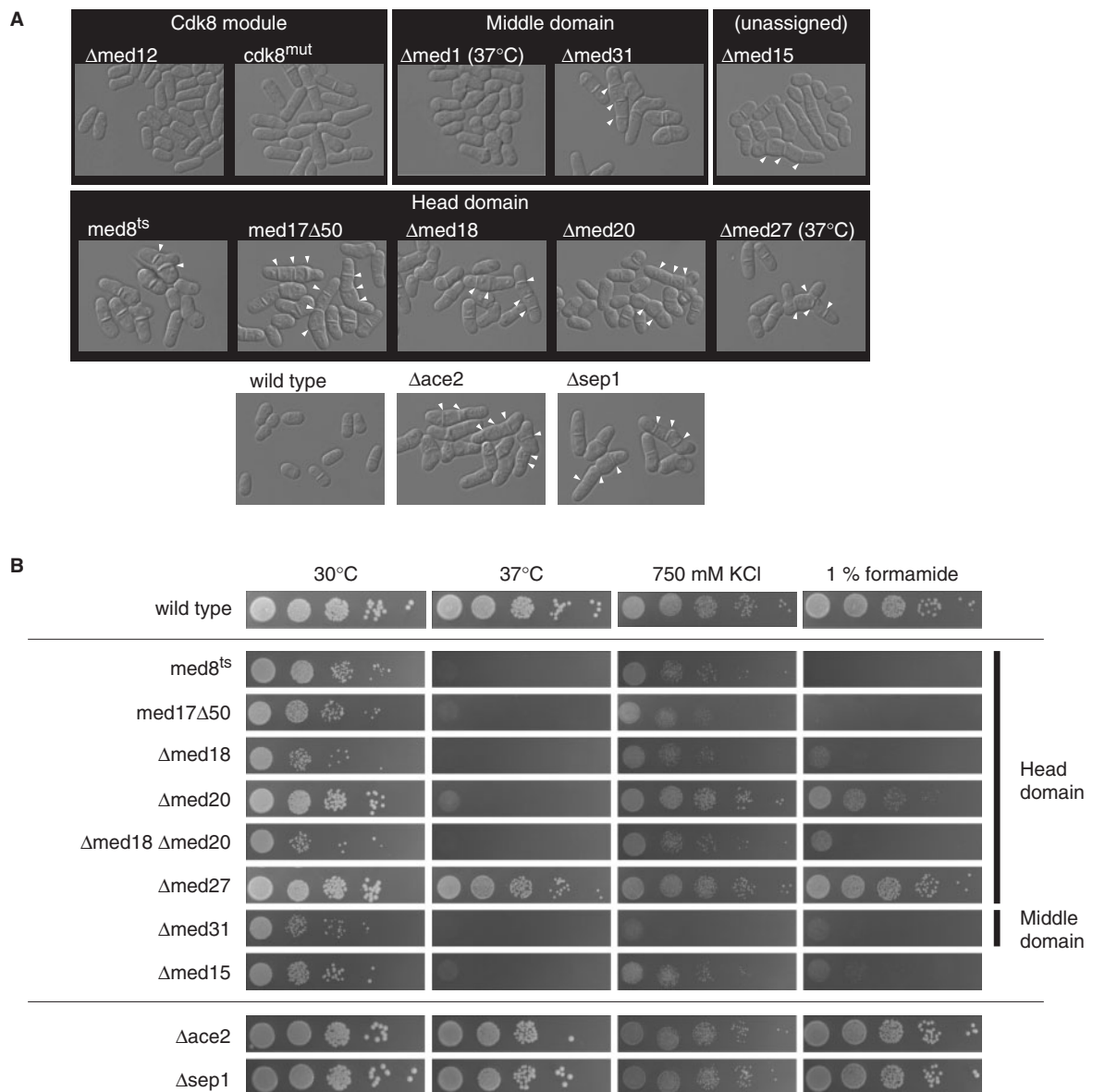


**Figure 3.** Phenotypes of *S. pombe* Mediator mutants. (A) Light microscopy of wild-type and mutant cells cultured in YES medium grown at 30°C unless otherwise indicated. Mediator mutants are organized according to their location within the Mediator. Unresolved septa are indicated by white arrows. The two well-characterized hyphal growth mutants *Ace2* and *Asep1* are included for comparison. (B) Ten-fold serial dilutions of wild-type and mutant cells under different forms of stress.

to each mutant that showed a 2-fold or more change in transcript levels—in total 531 genes.

### Mediator mutations elicit a partial stress response

Expression profiling of *S. cerevisiae* Mediator mutants have reported the increase of stress response gene transcript levels (46,53,55). We investigated whether this is also the case for *S. pombe* Mediator mutants. The central environmental stress response (CESR) in *S. pombe* consists of a set of genes whose transcript levels consistently increase or decrease during various forms of stress (38). The Affymetrix array platform used in our study contained 134 of the induced CESR genes.

We studied the occurrence of CESR genes above a defined fold change threshold and then calculated *P*-values using the hypergeometric probability distribution. We applied a 2-fold ratio change threshold for the *cdk8<sup>mut</sup>*, *Δmed12*, *Δmed18* and *Δmed20* datasets, while the large number of genes changing in the *Δmed15* and *med17Δ50* datasets required us to apply a 3-fold threshold in order to allow computation. The induced set of CESR genes were significantly overrepresented in the genes increasing their transcript levels above the threshold in all six datasets (Table 2, *P* < 0.001). In some mutants we also observed a significant overlap between downregulated genes and the genes belonging to the repressed set of CESR genes (data not shown). We confirmed the elevated transcription levels

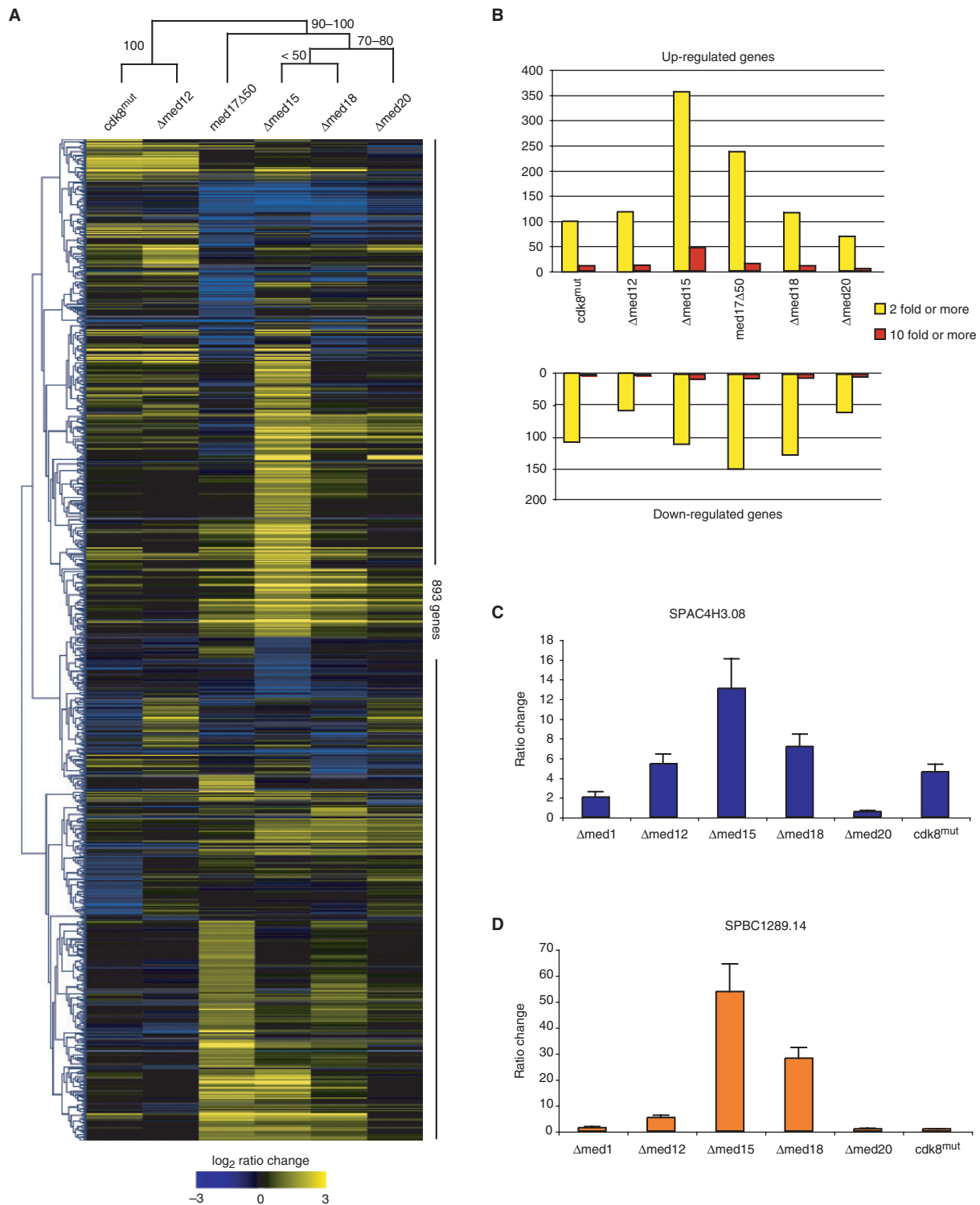


**Figure 4.** Genome-wide expression analysis of nonlethal *S. pombe* Mediator alleles. **(A)** Heatmap cluster diagram of the 893 transcripts that change 2-fold or more in at least one of the mutants. Experiments and genes were hierarchically clustered according to average Pearson correlation linkage. The robustness of the experimental dataset clusters were analyzed by bootstrap analysis in MeV using 10 000 replicates. Numbers on branches indicate the range of bootstrap values expressed as percentages. **(B)** Bar diagram showing the number of genes changing 2-fold or more (yellow bars) and 10-fold or more (red bars) in each mutant strain. **(C)** Quantitative real-time PCR analysis of SPAC4H3.08 transcript levels of the mutant strains indicated as compared to wild-type cells. SPAC4H3.08 levels were normalized to 28S rRNA. Error bars indicate 1 SD. **(D)** Quantitative real-time PCR analysis of SPBC1289.14 levels as described in (C).

**Table 2.** Occurrence of CESR transcripts in Mediator mutant expression profiles

Mutant	Fold-change cut-off	Increased transcripts	Induced CESR transcripts in the increased set
<i>cdk8<sup>mut</sup></i>	2	100	14 ( $p = 2.7 \times 10^{-7}$ )
<i>Amed12</i>	2	119	12 ( $p = 5.5 \times 10^{-5}$ )
<i>Amed15</i>	3	153	41 ( $p = 1.6 \times 10^{-31}$ )
<i>med17Δ50</i>	3	68	8 ( $p = 3.5 \times 10^{-4}$ )
<i>Amed18</i>	2	125	41 ( $p = 1.5 \times 10^{-35}$ )
<i>Amed20</i>	2	68	24 ( $p = 1.4 \times 10^{-21}$ )

of the two induced CESR genes SPAC4H3.08 and SPBC1289.14 by quantitative real-time PCR analysis (Figure 4C and D). These genes are known to become induced 10-fold or more following heat shock and hydrogen peroxide treatment, respectively (38). Although all strains tested showed at least a 2-fold increase in transcript levels, a substantially higher degree of upregulation of these two genes were observed in the *Amed15* mutant closely followed by the *Amed18* mutant. These observations taken together suggest a central role for Mediator in the regulation of some CESR genes. The actual molecular mechanism of this regulation remains to be elucidated.

#### Effects on genes involved in cell wall organization and metabolism

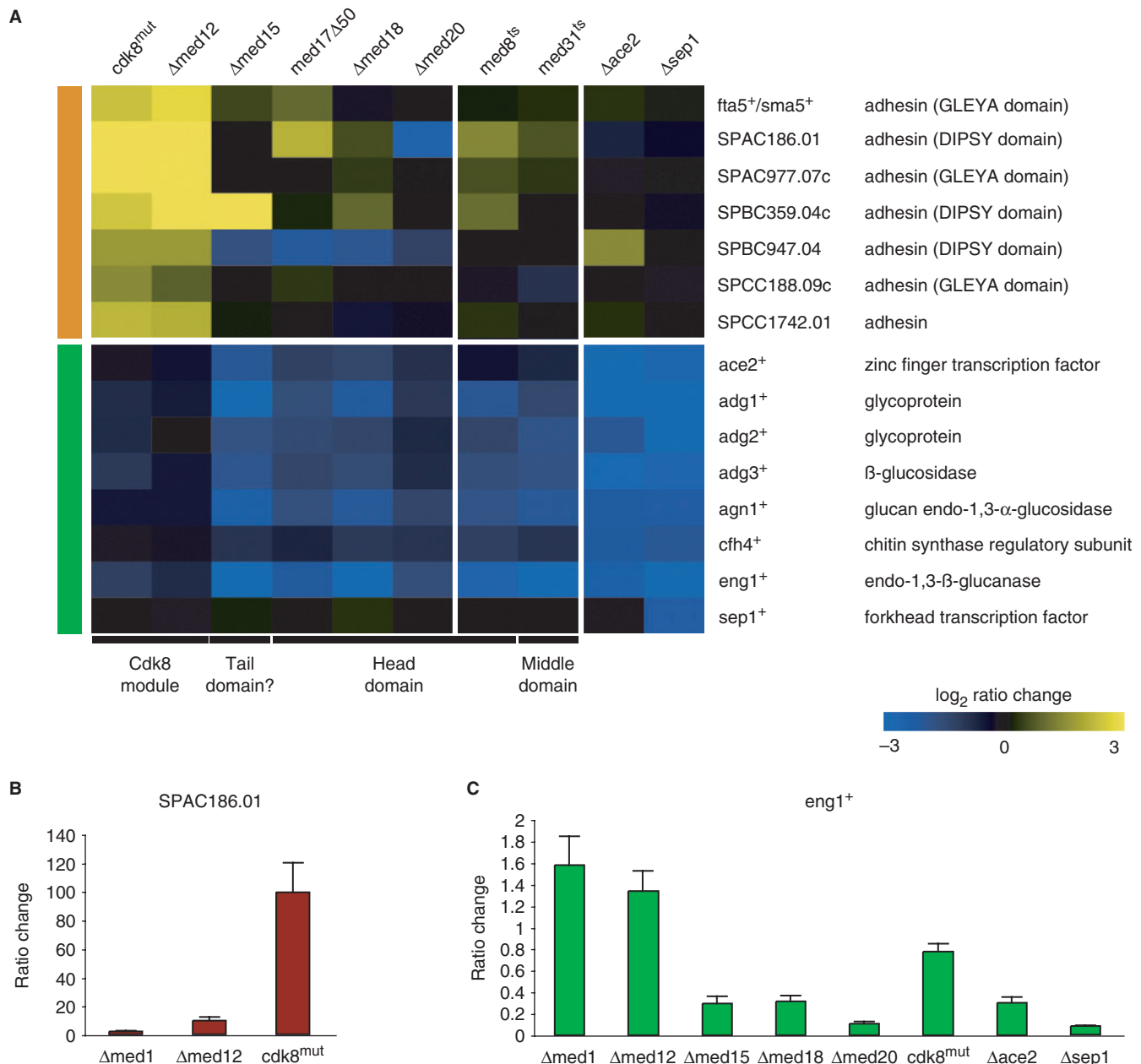
We looked specifically at genes annotated in the *S. pombe* genome database as being involved in cell wall metabolism to explain the clear morphological differences between mutants of the Cdk8 module and those of the core Mediator. Specifically, we investigated genes known or proposed to be involved in the process of cell-to-cell adhesion as well as postmitotic septum dissolution. We could discern two major groups of genes with distinct expression patterns. The first group consisted of a family of genes that code for putative cell surface adhesins (56). These adhesins displayed increased transcript levels in the *cdk8<sup>mut</sup>* and *Amed12* strains, but were largely unchanged in the head domain mutants (Figure 5A, orange bar). The increased transcript levels of these genes agree with the flocculation phenotype observed in *S. pombe* Cdk8 module mutants (Figure 3A) (10,48). The majority of the adhesin genes displayed only moderate increases in transcript levels (between 2- and 5-fold). One adhesin however, the DIPSY domain-containing SPAC186.01 gene, was upregulated nearly a 100-fold in the *cdk8<sup>mut</sup>* strain as assayed by quantitative real-time PCR (Figure 5B). This corresponded well with the stronger flocculation phenotype in this strain as compared to the somewhat milder phenotype observed for the *Amed12* mutant (data not shown). Some of the other members of the *S. pombe* adhesin family that displayed more moderate increases in transcript levels are related to the *FLO1*, *FLO5* and *FLO9* genes of *S. cerevisiae* (56). The *FLO* genes are known to be upregulated in *S. cerevisiae* Cdk8 module mutants as well (46,53,55) and we conclude that the role of the Cdk8 module as a repressor of Flo-like

adhesins appears conserved between *S. pombe* and *S. cerevisiae*.

The second group (Figure 5A, green bar) consisted of genes whose transcript levels were significantly decreased in the *Amed15* and head domain mutants, but with no significant change in the Cdk8 module mutants. This group included genes regulated by the transcription factor Ace2 as well as *ace2<sup>+</sup>* itself (37,51,57). These genes are expressed late in the cell cycle and involved the dissolution of the primary septum separating the newly formed daughter cells (51,57). Cells lacking these genes display septation defects. The Sep1 forkhead transcription factor regulates *ace2<sup>+</sup>* expression (37,57). Sep1 precedes Ace2 in the regulatory pathway and the *sep1<sup>+</sup>* gene was not affected by any of the mutants tested, suggesting that Sep1 requires the head domain subunits for *ace2<sup>+</sup>* transcription.

We also compared our profiles with published datasets of ts alleles of *med8<sup>+</sup>* and *med31<sup>+</sup>* (36). In agreement with their hyphal phenotypes only the Ace2-regulated genes were affected in these two mutants. Likewise, *Δace2* and *Δsep1* expression data (37) did not exhibit any significant changes in expression of surface adhesins indicating that the Cdk8 module does not play a role in the expression of Ace2-dependent genes. The *ace2<sup>+</sup>*-regulated *eng1<sup>+</sup>* gene encodes an endoglucanase that is required for the dissolution of the primary division septum following mitosis, and its deletion leads to a septation phenotype similar to that of *Δace2* and *Δsep1* cells (51). We performed quantitative real-time PCR analysis of *eng1<sup>+</sup>* transcript levels in the Mediator mutants and the *Δace2* and *Δsep1* strains to directly compare the magnitude of decrease in this particular gene. We observed that the decrease in the head domain mutants and *Amed15* was equivalent to that of the *Δace2* and *Δsep1* mutants (Figure 5C). We therefore conclude that the *S. pombe* Mediator head domain and Med15 subunit play a crucial role in the transcription of *ace2<sup>+</sup>/sep1<sup>+</sup>*-dependent genes. We would like to point out that this analysis was done on asynchronous cells and therefore does not reveal any potential effect on the timing of cell cycle-dependent expression patterns.

Degradation of the primary septum in *S. cerevisiae* is controlled in part by the *ACE2* gene, the homolog of *S. pombe ace2<sup>+</sup>* (58,59). However, primary septum dissolution and cell separation is fundamentally different and most of the required factors lack *S. pombe* homologs (60,61). Nevertheless, quantitative real-time PCR analysis of three genes wholly or partially regulated by *S. cerevisiae ACE2-AMN1/CTS13*, *DSE2* and *DSE4/ENG1* (58,59) all displayed decreased transcript levels in head and tail domain mutants compared to wild-type cells when grown in rich medium (Figure 6). Analysis of previously published expression data for *S. cerevisiae* Mediator mutants grown in minimal media revealed that this effect can be observed in other *ACE2*-regulated genes as well (53). We therefore conclude that the requirement of the head and tail domain for Ace2-dependent expression appears conserved between *S. pombe* and *S. cerevisiae*.



## DISCUSSION

In this study, we use a combined genetic and biochemical approach to perform a functional characterization of the *S. pombe* Mediator complex. Our data suggest a head module architecture with a stepwise structural organization: Med27 located on the very exterior connected to Med20, which in turn contacts Med18 which binds Med8 (Figure 1E). Biochemical characterization of the *med17Δ50* allele suggested that Med17 may act as scaffold

for the head domain subunits and this function requires an intact C-terminus of the Med17 subunit (Figure 2C and D).

Removal of Med27 does not affect the association of Med18 or Med20 with Mediator to any detectable extent (Figure 1D). In addition, *Δmed27* cells do not display visible phenotypes unless heat stressed (Figure 3A) and appear only marginally less stress tolerant than wild-type cells (Figure 3B). Removal of Med20 also caused the

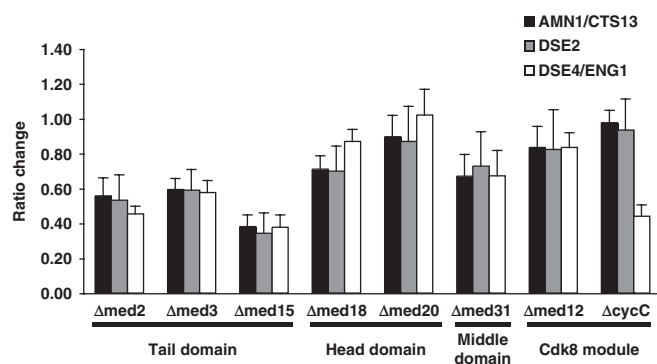


**Figure 6.** The requirement of the Mediator head and tail domain for Ace2-dependent transcription in *S. cerevisiae*. Quantitative real-time PCR analysis of transcript levels of the indicated mutant strains as compared to wild-type cells. Transcript levels for all genes were normalized to *TUB1* in accordance with previous studies of *S. cerevisiae* Mediator mutants (53).

complete loss of Med27 as well as an apparent decrease in the amount of Med18 (Figure 1C). A corresponding increase in severity is observed both in the cellular morphology of *Amed20* cells (Figure 3A) as well as their stress tolerance (Figure 3B). The strongest effect was seen in *Amed18* Mediator where both Med20 and Med27 were lost (Figure 1C). Similarly, the *Amed18* phenotype was more severe than that of *Amed20* cells. A *Amed18 Amed20* double mutant appeared indistinguishable from a *Amed18* strain at 30°C demonstrating that *med18* is epistatic to *med20*. This is what we would expect as Med20 is unable to associate with *Amed18* Mediator (Figure 1C). Consolidation of the biochemical data with the observed phenotypes indicated that the loss of Med18, which occurred in *Amed18* (Figure 1C) and *med8<sup>ts</sup>* cells (Figure 1D) as well as *med17Δ50* cells cultured above room temperature (Figure 2C), appeared sufficient to cause the septation defect and stress hypersensitivity. The somewhat milder phenotype in *Amed20* cell may well be caused by a decrease in the number of Med18 containing Mediator in the *Amed20* cells (Figure 1C) rather than the loss of the Med20 subunit in itself.

The Med17 subunit has played a key role in establishing the almost absolute requirement for Mediator in pol II-dependent transcription in *S. cerevisiae* (45,46). The conditional *S. pombe med17Δ50* allele isolated in this study is different to the *S. cerevisiae srb4-138* allele in several respects. First, the *S. pombe med17Δ50* allele is a C-terminally truncated form while the *srb4-138* allele has a number of single nucleotide substitutions along the entire coding region (62). Second, we do not see an equally rapid growth arrest at the nonpermissive temperature in *S. pombe* (Figure 2A) as reported in the *S. cerevisiae* mutant (45). The growth arrest in *S. cerevisiae* appears directly linked to the immediate cessation of pol II-dependent transcription as the Mediator complex comes apart (19). The effect on Mediator stability in *S. pombe med17Δ50* is less clear-cut with an increase in severity at higher temperatures (Figure 2C and D). We also observed that transcription does not shut down

globally at the nonpermissive temperature in *S. pombe med17Δ50* cells (Figure 2B). In addition, global chromatin immunoprecipitation of *med17Δ50* Mediator showed a clear pattern of genomic reorganization after heat shock rather than a global reduction of Mediator binding (63).

In this work, we addressed the function of the potential *S. pombe* Mediator subunit Med15. Our data clearly demonstrate a functional link between Med15 and Mediator. Specifically, the phenotype and transcript profile of *Amed15* cells links Med15 to the head domain and to the middle domain subunit Med31 (Figures 3A and 4A). Presently, we do not know whether Med15 is able to stably associate with Mediator.

A relatively large number of core environmental stress-related (CESR) transcripts changed significantly in the expression profiles of all six Mediator mutants analyzed in this study. We interpret these data as the result of either one of two scenarios. First, the mutation might perturb cellular homeostasis to such a degree that the stress response is triggered as a secondary effect of the respective mutation. Alternatively, Mediator components could act as direct regulators of the stress response and so by removal of the regulator, the transcriptional program is triggered inadvertently. Further work will be required to shed light on this observation. However, Cdk8 in *S. cerevisiae* is known to specifically phosphorylate transcription factors directly involved in stress gene regulation (64), which therefore also would implicate Mediator as a direct regulator of the cellular stress response.

Expression profiles of genes known to be involved in cell wall metabolism correlated very well with the aberrant cellular morphologies observed in *S. pombe* Mediator mutants (Figures 3A and 5A–C). The flocculation phenotype seen in Cdk8 module mutants was likely the result of overproduction of surface adhesins (Figure 5A and B), a typical stress response in yeast and regulated by stress-related pathways such as MAP kinase cascades (47). Deletion of Cdk8 module genes in *S. cerevisiae* also leads to flocculation (46,65,66), suggesting that regulation of adhesins is conserved between *S. pombe* and *S. cerevisiae*. Indeed, transcript levels of the *S. cerevisiae* adhesin-coding genes *FLO1*, *FLO5* and *FLO9* are significantly elevated in Cdk8 module mutants (53,67).

Conversely, the decreased expression of genes involved in the degradation of primary septum would explain the hyphal growth in head domain mutants and the *Amed15* strain. Although transcription was not completely abolished the cumulative effect of several downregulated genes might give rise to the hyphal growth. The process of septum dissolution to achieve complete cell separation is fundamentally different between *S. pombe* and *S. cerevisiae* (49,60). In *S. pombe* the primary septum consists of 1,3-β-glucan which is primarily degraded by the Eng1 endoglucanase (51) while in *S. cerevisiae* the primary septum is made up of chitin and is subsequently degraded by the Cts1 endochitinase (51). The cell wall material surrounding the septum, the so-called septum edging, also differs in its composition between the two species. In *S. pombe* it is mainly composed of 1,3-α-glucan that is degraded by the Agn1 endoglucanase (68). In *S. cerevisiae*, the septum edging is 1,3-β-glucan and degraded by the

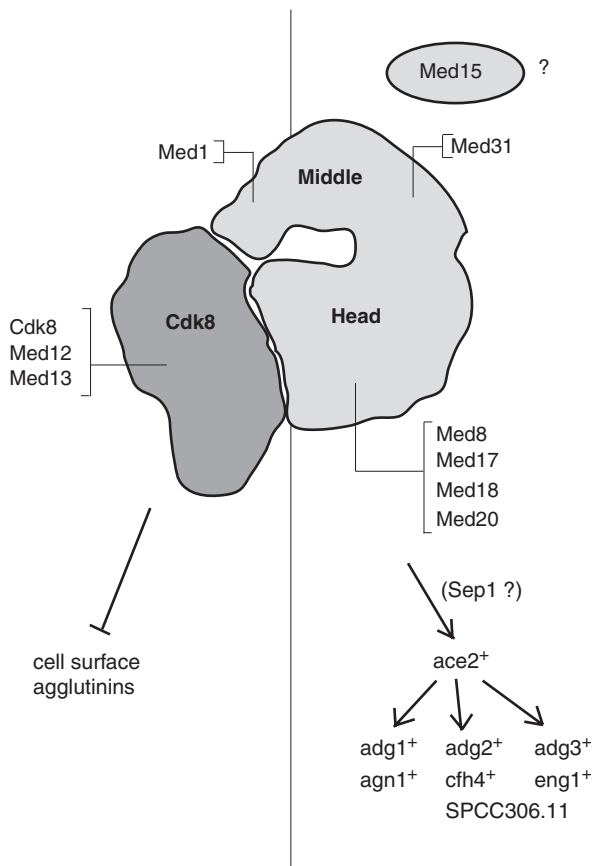


**Figure 7.** Two classes of nonessential mutant alleles in fission yeast Mediator. A diagram of *S. pombe* L-Mediator based on single-particle EM structures (11). The functional data presented in this work allow us to draw a virtual line through the Mediator. To the left are components of the Cdk8 module and the middle domain subunit Med1. When deleted these cells aggregate due to the overexpression of adhesive surface proteins as outlined in the text. To the right are mutant alleles of the head domain as well as the nonessential middle domain subunit Med31 and the Med15 factor. These mutants have a hyphal growth defect due to the faulty expression of genes required for efficient cell separation.

Eng1 endo-glucanase (61,69). The process is regulated by the conserved Ace2 transcription factor in both species but most of the target genes are not conserved between *S. pombe* and *S. cerevisiae*. We were therefore quite struck by the fact that the Mediator head domain and tail domain (only the Med15 subunit in *S. pombe*) were required for proper expression of Ace2-dependent genes in both *S. pombe* and *S. cerevisiae* despite the many differences in the process (Figures 5A and 6) (53). Even though the tail domain is not conserved in *S. pombe*, the Med15 protein still has an essential role to play in the Ace2-regulated septation cascade.

In summary, the data presented in this article suggest a structural model for the *S. pombe* head domain and clearly defines two distinct functional classes of subunits within the *S. pombe* Mediator complex (Figure 7). The first class consists of all four components of the Cdk8 module as well as middle domain subunit Med1. If deleted, this group all flocculate due to de-repression of cell surface adhesions, some of which may be involved in

mating, stress response or adaptation to starvation conditions. The second class is composed of the head domain as well as middle domain subunit Med31 and the as yet unassigned Med15 protein. When mutated these genes cause septation defects leading to hyphal growth due to impaired expression of the Ace2-dependent genes involved in cell separation. Our results and previously published expression data indicate that the head domain, Med31 and Med15 are required for the proper expression of the *ace2*<sup>+</sup> gene, possibly by the Sep1 transcription factor. Thus, our work identifies two distinct functional submodules of the *S. pombe* Mediator that have conserved roles in the regulation of specific cellular pathways.

## SUPPLEMENTARY DATA

Supplementary Data are available at NAR Online.

## ACKNOWLEDGEMENTS

We are very grateful to the labs of Stefan Björklund, Frans Hochstenbach, Roger Kornberg, Matthias Sipiczki and Richard A. Young for the generous gifts of yeast strains and antibodies. Valerie Wood of the Sanger Centre *Schizosaccharomyces pombe* sequence database was very helpful in providing functional annotations and tables of *S. cerevisiae* orthologs for *S. pombe* genes as well as answering any questions we had. We are also very grateful to David Brodin of the Huddinge Affymetrix Facility for assistance with the expression analysis. C.M.G. was supported by grants from the Swedish Research Council, the Swedish Cancer Society and the Swedish Foundation for Strategic Research. S.H. was supported by grants from the Danish Research Councils and Manufacturer Vilhelm Pedersen and Wife Memorial Legacy (this support was granted on recommendation from the Novo Nordisk Foundation). Funding to pay the Open Access publication charges for this article was provided by the Danish Research Councils.

*Conflict of interest statement.* None declared.

## REFERENCES

- Björklund, S. and Gustafsson, C.M. (2005) The yeast Mediator complex and its regulation. *Trends Biochem. Sci.*, **30**, 240–244.
- Kelleher, R.J., III, Flanagan, P.M. and Kornberg, R.D. (1990) A novel mediator between activator proteins and the RNA polymerase II transcription apparatus. *Cell*, **61**, 1209–1215.
- Flanagan, P.M., Kelleher, R.J., III, Sayre, M.H., Tschochner, H. and Kornberg, R.D. (1991) A mediator required for activation of RNA polymerase II transcription in vitro. *Nature*, **350**, 436–438.
- Conaway, J.W., Florens, L., Sato, S., Tomomori-Sato, C., Parmely, T.J., Yao, T., Swanson, S.K., Banks, C.A., Washburn, M.P. and Conaway, R.C. (2005) The mammalian Mediator complex. *FEBS Lett.*, **579**, 904–908.
- Conaway, R.C., Sato, S., Tomomori-Sato, C., Yao, T. and Conaway, J.W. (2005) The mammalian Mediator complex and its role in transcriptional regulation. *Trends Biochem. Sci.*, **30**, 250–255.
- Spahr, H., Samuelsen, C.O., Baraznenok, V., Ernest, I., Huylebroeck, D., Remacle, J.E., Samuelsson, T., Kieselbach, T., Holmberg, S. and Gustafsson, C.M. (2001) Analysis of *Schizosaccharomyces pombe* Mediator reveals a set of essential

- subunits conserved between yeast and metazoan cells. *PNAS*, **98**, 11985–11990.
7. Boube, M., Joulia, L., Cribbs, D.L. and Bourbon, H.M. (2002) Evidence for a mediator of RNA polymerase II transcriptional regulation conserved from yeast to man. *Cell*, **110**, 143–151.
  8. Bourbon, H.M., Aguilera, A., Ansari, A.Z., Asturias, F.J., Berk, A.J., Bjorklund, S., Blackwell, T.K., Borggreffe, T., Carey, M., Carlson, M. *et al.* (2004) A unified nomenclature for protein subunits of mediator complexes linking transcriptional regulators to RNA polymerase II. *Mol. Cell*, **14**, 553–557.
  9. Spahr, H., Beve, J., Larsson, T., Bergstrom, J., Karlsson, K.A. and Gustafsson, C.M. (2000) Purification and characterization of RNA polymerase II holoenzyme from *Schizosaccharomyces pombe*. *J. Biol. Chem.*, **275**, 1351–1356.
  10. Samuelsen, C.O., Baraznenok, V., Khorosjutina, O., Spahr, H., Kieselbach, T., Holmberg, S. and Gustafsson, C.M. (2003) TRAP230/ARC240 and TRAP240/ARC250 Mediator subunits are functionally conserved through evolution. *PNAS*, **100**, 6422–6427.
  11. Elmlund, H., Baraznenok, V., Lindahl, M., Samuelsen, C.O., Koek, P.J., Holmberg, S., Hebert, H. and Gustafsson, C.M. (2006) The cyclin-dependent kinase 8 module sterically blocks Mediator interactions with RNA polymerase II. *Proc. Natl Acad. Sci. USA*, **103**, 15788–15793.
  12. Borggreffe, T., Davis, R., Erdjument-Bromage, H., Tempst, P. and Kornberg, R.D. (2002) A complex of the *srb8*, *-9*, *-10*, and *-11* transcriptional regulatory proteins from yeast. *J. Biol. Chem.*, **277**, 44202–44207.
  13. Hengartner, C.J., Myer, V.E., Liao, S.M., Wilson, C.J., Koh, S.S. and Young, R.A. (1998) Temporal regulation of RNA polymerase II by *Srb10* and *Kin28* cyclin-dependent kinases. *Mol. Cell*, **2**, 43–53.
  14. Spahr, H., Khorosjutina, O., Baraznenok, V., Linder, T., Samuelsen, C.O., Hermand, D., Makela, T.P., Holmberg, S. and Gustafsson, C.M. (2003) Mediator Influences *Schizosaccharomyces pombe* RNA polymerase II-dependent transcription in vitro. *J. Biol. Chem.*, **278**, 51301–51306.
  15. Hirst, M., Kobar, M.S., Kuriakose, N., Greenblatt, J. and Sadowski, I. (1999) GAL4 is regulated by the RNA polymerase II holoenzyme-associated cyclin-dependent protein kinase *SRB10/CDK8*. *Mol. Cell*, **3**, 673–678.
  16. Larschan, E. and Winston, F. (2005) The *Saccharomyces cerevisiae* *Srb8-Srb11* complex functions with the SAGA complex during Gal4-activated transcription. *Mol. Cell Biol.*, **25**, 114–123.
  17. Asturias, F.J., Jiang, Y.W., Myers, L.C., Gustafsson, C.M. and Kornberg, R.D. (1999) Conserved structures of mediator and RNA polymerase II holoenzyme. *Science*, **283**, 985–987.
  18. Davis, J.A., Takagi, Y., Kornberg, R.D. and Asturias, F.J. (2002) Structure of the yeast RNA polymerase II holoenzyme: Mediator conformation and polymerase interaction. *Mol. Cell*, **10**, 409–415.
  19. Linder, T., Zhu, X., Baraznenok, V. and Gustafsson, C.M. (2006) The classical *srb4-138* mutant allele causes dissociation of yeast Mediator. *Biochem. Biophys. Res. Commun.*, **349**, 948–953.
  20. Lee, Y.C. and Kim, Y.-J. (1998) Requirement for a functional interaction between Mediator components *Med6* and *Srb4* in RNA polymerase II transcription. *Mol. Cell Biol.*, **18**, 5364–5370.
  21. Lee, Y.C., Park, J.M., Min, S., Han, S.J. and Kim, Y.J. (1999) An activator binding module of yeast RNA polymerase II holoenzyme. *Mol. Cell Biol.*, **19**, 2967–2976.
  22. Kang, J.S., Kim, S.H., Hwang, M.S., Han, S.J., Lee, Y.C. and Kim, Y.J. (2001) The structural and functional organization of the yeast mediator complex. *J. Biol. Chem.*, **276**, 42003–42010.
  23. Guglielmi, B., van Berkum, N.L., Klapholz, B., Bijma, T., Boube, M., Boschiero, C., Bourbon, H.-M., Holstege, F.C.P. and Werner, M. (2004) A high resolution protein interaction map of the yeast Mediator complex. *Nucleic Acids Res.*, **32**, 5379–5391.
  24. Koh, S.S., Ansari, A.Z., Ptashne, M. and Young, R.A. (1998) An activator target in the RNA polymerase II holoenzyme. *Mol. Cell*, **1**, 895–904.
  25. Takagi, Y. and Kornberg, R.D. (2006) Mediator as a general transcription factor. *J. Biol. Chem.*, **281**, 80–89.
  26. Krawchuk, M.D. and Wahls, W.P. (1999) High-efficiency gene targeting in *Schizosaccharomyces pombe* using a modular, PCR-based approach with long tracts of flanking homology. *Yeast*, **15**, 1419–1427.
  27. MacIver, F.H., Glover, D.M. and Hagan, I.M. (2003) A 'marker switch' approach for targeted mutagenesis of genes in *Schizosaccharomyces pombe*. *Yeast*, **20**, 587–594.
  28. Forsburg, S.L. (1993) Comparison of *Schizosaccharomyces pombe* expression systems. *Nucleic Acids Res.*, **21**, 2955–2956.
  29. Hashimoto, T. and Sekiguchi, M. (1976) Isolation of temperature-sensitive mutants of R plasmid by in vitro mutagenesis with hydroxylamine. *J. Bacteriol.*, **127**, 1561–1563.
  30. Rigaut, G. (1999) A generic protein purification method for protein complex characterization and proteome exploration. *Nat. Biotechnol.*, **17**, 1030–1032.
  31. Puig, O. (2001) The tandem affinity purification (TAP) method: a general procedure of protein complex purification. *Methods*, **24**, 218–229.
  32. Linder, T. and Gustafsson, C.M. (2004) The *Soh1/MED31* Protein is an ancient component of *Schizosaccharomyces pombe* and *Saccharomyces cerevisiae* Mediator. *J. Biol. Chem.*, **279**, 49455–49459.
  33. Schmitt, M.E., Brown, T.A. and Trumpower, B.L. (1990) A rapid and simple method for preparation of RNA from *Saccharomyces cerevisiae*. *Nucleic Acids Res.*, **18**, 3091–3092.
  34. Affymetrix (2004) *GeneChip Expression Analysis - Technical Manual*.
  35. Saeed, A.I., Sharov, V., White, J., Li, J., Liang, W., Bhagabati, N., Braisted, J., Klapa, M., Currier, T., Thiagarajan, M. *et al.* (2003) TM4: a free, open-source system for microarray data management and analysis. *Biotechniques*, **34**, 374–378.
  36. Miklos, I., Szilagy, Z., Watt, S., Zilahi, E., Batta, G., Antunovics, Z., Enczi, K., Bahler, J. and Sipiczki, M. (2008) Genomic expression patterns in cell separation mutants of *Schizosaccharomyces pombe* defective in the genes *sep10 (+)* and *sep15 (+)* coding for the Mediator subunits *Med31* and *Med8*. *Mol. Genet. Genomics*, **279**, 225–238.
  37. Rustici, G., Mata, J., Kivinen, K., Lio, P., Penkett, C.J., Burns, G., Hayles, J., Brazma, A., Nurse, P. and Bahler, J. (2004) Periodic gene expression program of the fission yeast cell cycle. *Nat. Genet.*, **36**, 809–817.
  38. Chen, D., Toone, W.M., Mata, J., Lyne, R., Burns, G., Kivinen, K., Brazma, A., Jones, N. and Bahler, J. (2003) Global transcriptional responses of fission yeast to environmental stress. *Mol. Biol. Cell*, **14**, 214–229.
  39. Moreira, J.M. and Holmberg, S. (1998) Nucleosome structure of the yeast *CHA1* promoter: analysis of activation-dependent chromatin remodeling of an RNA-polymerase-II-transcribed gene in TBP and RNA pol II mutants defective in vivo in response to acidic activators. *EMBO J.*, **17**, 6028–6038.
  40. Lariviere, L., Geiger, S., Hoepfner, S., Rother, S., Straszer, K. and Cramer, P. (2006) Structure and TBP binding of the Mediator head subcomplex *Med8-Med18-Med20*. **13**, 895–901.
  41. Szilagy, Z., Grallert, A., Nemeth, N. and Sipiczki, M. (2002) The *Schizosaccharomyces pombe* genes *sep10* and *sep11* encode putative general transcriptional regulators involved in multiple cellular processes. *Mol. Genet. Genomics*, **268**, 553–562.
  42. Zilahi, E., Miklos, I. and Sipiczki, M. (2000) The *Schizosaccharomyces pombe* *sep15+* gene encodes a protein homologous to the *Med8* subunit of the *Saccharomyces cerevisiae* transcriptional mediator complex. *Curr. Genet.*, **38**, 227–232.
  43. Garcia-Gimeno, M.A., Munoz, I., Arino, J. and Sanz, P. (2003) Molecular characterization of *Ypi1*, a novel *Saccharomyces cerevisiae* type I protein phosphatase inhibitor. *J. Biol. Chem.*, **278**, 47744–47752.
  44. Grallert, A., Grallert, B., Zilahi, E., Szilagy, Z. and Sipiczki, M. (1999) Eleven novel *sep* genes of *Schizosaccharomyces pombe* required for efficient cell separation and sexual differentiation. *Yeast*, **15**, 669–686.
  45. Thompson, C.M. and Young, R.A. (1995) General requirement for RNA polymerase II holoenzymes in vivo. *Proc. Natl Acad. Sci. USA*, **92**, 4587–4590.
  46. Holstege, F.C., Jennings, E.G., Wyrick, J.J., Lee, T.I., Hengartner, C.J., Green, M.R., Golub, T.R., Lander, E.S. and Young, R.A. (1998) Dissecting the regulatory circuitry of a eukaryotic genome. *Cell*, **95**, 717–728.
  47. Verstrepen, K.J. and Klis, F.M. (2006) Flocculation, adhesion and biofilm formation in yeasts. *Mol. Microbiol.*, **60**, 5–15.

48. Watson, P. and Davey, J. (1998) Characterization of the Prk1 protein kinase from *Schizosaccharomyces pombe*. *Yeast*, **14**, 485–492.
49. Feierbach, B. and Chang, F. (2001) Cytokinesis and the contractile ring in fission yeast. *Curr. Opin. Microbiol.*, **4**, 713–719.
50. Sipiczki, M., Grallert, B. and Miklos, I. (1993) Mycelial and syncytial growth in *Schizosaccharomyces pombe* induced by novel septation mutations. *J. Cell Sci.*, **104**(Pt 2), 485–493.
51. Martin-Cuadrado, A.B., Duenas, E., Sipiczki, M., Vazquez de Aldana, C.R. and del Rey, F. (2003) The endo-beta-1,3-glucanase eng1p is required for dissolution of the primary septum during cell separation in *Schizosaccharomyces pombe*. *J. Cell Sci.*, **116**, 1689–1698.
52. Ribar, B., Banrevi, A. and Sipiczki, M. (1997) sep1+ encodes a transcription-factor homologue of the HNF-3/forkhead DNA-binding-domain family in *Schizosaccharomyces pombe*. *Gene*, **202**, 1–5.
53. van de Peppel, J., Kettlerij, N., van Bakel, H., Kockelkorn, T.T., van Leenen, D. and Holstege, F.C. (2005) Mediator expression profiling epistasis reveals a signal transduction pathway with antagonistic submodules and highly specific downstream targets. *Mol. Cell*, **19**, 511–522.
54. Eisen, M.B., Spellman, P.T., Brown, P.O. and Botstein, D. (1998) Cluster analysis and display of genome-wide expression patterns. *Proc. Natl Acad. Sci. USA*, **95**, 14863–14868.
55. Chang, Y.-W., Howard, S.C. and Herman, P.K. (2004) The Ras/PKA signaling pathway directly targets the srb9 protein, a component of the general RNA polymerase II transcription apparatus. *Mol. Cell*, **15**, 107–116.
56. Linder, T. and Gustafsson, C.M. (2007) Molecular phylogenetics of ascomycotal adhesins - A novel family of putative cell-surface adhesive proteins in fission yeasts. *Fungal Genet. Biol.* doi:10.1016/j.fgb.2007.08.002 [Epub ahead of print].
57. Alonso-Nunez, M.L., An, H., Martin-Cuadrado, A.B., Mehta, S., Petit, C., Sipiczki, M., del Rey, F., Gould, K.L. and de Aldana, C.R. (2005) Ace2p controls the expression of genes required for cell separation in *Schizosaccharomyces pombe*. *Mol. Biol. Cell*, **16**, 2003–2017.
58. Colman-Lerner, A., Chin, T.E. and Brent, R. (2001) Yeast Cbk1 and Mob2 activate daughter-specific genetic programs to induce asymmetric cell fates. *Cell*, **107**, 739–750.
59. Doolin, M.T., Johnson, A.L., Johnston, L.H. and Butler, G. (2001) Overlapping and distinct roles of the duplicated yeast transcription factors Ace2p and Swi5p. *Mol. Microbiol.*, **40**, 422–432.
60. Yeong, F.M. (2005) Severing all ties between mother and daughter: cell separation in budding yeast. *Mol. Microbiol.*, **55**, 1325–1331.
61. Cabib, E., Roh, D.H., Schmidt, M., Crotti, L.B. and Varma, A. (2001) The yeast cell wall and septum as paradigms of cell growth and morphogenesis. *J. Biol. Chem.*, **276**, 19679–19682.
62. Takagi, Y., Calero, G., Komori, H., Brown, J.A., Ehrensberger, A.H., Hudmon, A., Asturias, F. and Kornberg, R.D. (2006) Head module control of mediator interactions. *Mol. Cell*, **23**, 355–364.
63. Zhu, X., Wiren, M., Sinha, I., Rasmussen, N.N., Linder, T., Holmberg, S., Ekwall, K. and Gustafsson, C.M. (2006) Genome-wide occupancy profile of mediator and the Srb8-11 module reveals interactions with coding regions. *Mol. Cell*, **22**, 169–178.
64. Chi, Y., Huddleston, M.J., Zhang, X., Young, R.A., Annan, R.S., Carr, S.A. and Deshaies, R.J. (2001) Negative regulation of Gcn4 and Msn2 transcription factors by Srb10 cyclin-dependent kinase. *Genes Dev.*, **15**, 1078–1092.
65. Nelson, C., Goto, S., Lund, K., Hung, W. and Sadowski, I. (2003) Srb10/Cdk8 regulates yeast filamentous growth by phosphorylating the transcription factor Ste12. *Nature*, **421**, 187–190.
66. Chang, Y.W., Howard, S.C., Budovskaya, Y.V., Rine, J. and Herman, P.K. (2001) The rye mutants identify a role for Ssn/Srb proteins of the RNA polymerase II holoenzyme during stationary phase entry in *Saccharomyces cerevisiae*. *Genetics*, **157**, 17–26.
67. Chang, Y.W., Howard, S.C. and Herman, P.K. (2004) The Ras/PKA signaling pathway directly targets the Srb9 protein, a component of the general RNA polymerase II transcription apparatus. *Mol. Cell*, **15**, 107–116.
68. Dekker, N., Speijer, D., Grun, C.H., van den Berg, M., de Haan, A. and Hochstenbach, F. (2004) Role of the alpha-glucanase Agn1p in fission-yeast cell separation. *Mol. Biol. Cell*, **15**, 3903–3914.
69. Baladron, V., Ufano, S., Duenas, E., Martin-Cuadrado, A.B., del Rey, F. and Vazquez de Aldana, C.R. (2002) Eng1p, an endo-1,3-beta-glucanase localized at the daughter side of the septum, is involved in cell separation in *Saccharomyces cerevisiae*. *Eukaryot. Cell*, **1**, 774–786.